Charge-dependent transverse momentum and its impact on the search for the chiral magnetic wave

Wen-Ya Wu,[1] Chun-Zheng Wang,[2,3] Qi-Ye Shou ●,[1,*] Yu-Gang Ma,[1,2,†] and Liang Zheng ●[4]

[1]*Key Laboratory of Nuclear Physics and Ion-beam Application (MOE), Institute of Modern Physics, Fudan University, Shanghai 200433, China*

[2]*Shanghai Institute of Applied Physics, Chinese Academy of Sciences, Shanghai 201800, China*

[3]*University of Chinese Academy of Sciences, Beijing 100049, China*

[4]*School of Mathematics and Physics, China University of Geosciences (Wuhan), Wuhan 430074, China*

The chiral magnetic wave (CMW) is sought using the charge asymmetry (A_{ch}) dependence of anisotropic flow in heavy-ion collisions. The charge-dependent transverse momentum (p_T), however, could play a role as a background. With the string fragmentation models, including PYTHIA, we demonstrate the origin of the A_{ch}-p_T correlation and its connection with the local charge conservation (LCC). The impact of A_{ch}-p_T and its behavior in varied kinematic windows are also discussed. This study provides more insights for the search for the CMW and comprehending the collective motion of the quark-gluon plasma.

I. INTRODUCTION

In relativistic heavy-ion collisions, the interplay of the chiral anomaly and the intense magnetic field created in off-central collisions is proposed to generate several kinds of anomalous chiral phenomena [1–4], e.g., the chiral magnetic effect (CME), the chiral separation effect (CSE), and the chiral magnetic wave (CMW) [5–8]. While the CME could manifest itself in a finite electric dipole moment with respect to the reaction plane [9], the CMW is expected to generate an electric quadrupole moment in the quark-gluon plasma (QGP), where the "poles" (out of plane) and the "equator" (in plane) of the participant region respectively acquire additional positive or negative charges. Taking advantage of the anisotropic emission of particles in the azimuthal direction, it is feasible to measure the CMW using the charge asymmetry (A_{ch}) dependence of elliptic flow (v_2) between the positively and negatively charged particles, i.e.,

$$\Delta v_2 \equiv v_2^- - v_2^+ \simeq r A_{ch}, \qquad (1)$$

where $A_{ch} \equiv (N^+ - N^-)/(N^+ + N^-)$ with N denoting the number of particles in a given event, and the slope r is used to quantify the strength. Phenomenological simulations [10,11] confirm that the charge separation caused by the CMW is bound to bring about this linear dependence.

Over the past decade, the STAR [12,13], ALICE [14], and CMS [15] collaborations have performed the measurements at various collision energies and systems. A robust relationship between v_2 and A_{ch} is observed and the slope extracted at semicentral collisions agrees with the theoretical expectation, seemingly bearing out the CMW theory. Nevertheless, the strikingly similar linear relation is also experimentally observed in p-Pb collisions and for triangular flow (v_3) [15].

The direction of the magnetic field is irrelevant to the reaction plane in small system collisions [16,17] and the quadrupole configuration is unable to cause the A_{ch}-v_3 relation. For that reason, one can assert the existence of the non-CMW background.

Understanding the components of the background and how they contribute to the observable are essential to disentangle the CMW signal. Among several sources [18–24], the most important one is suggested to be the local charge conservation (LCC) entwined with the collective motion of the QGP. Reference [18] introduces the LCC effect into a hydrodynamic model, which can qualitatively generate the linear relation between v_2 and A_{ch}, albeit with a smaller slope compared to the data. Reference [19] demonstrates some basic features of the LCC with a simple blast wave model and proposes a novel observable, three-particle correlator. Both of these two studies mimic the LCC by forcing the charged particles to emit always in pairs (one positively and one negatively charged) at the same spatial point. On the other hand, without artificially introducing the charge-conserving pair, AMPT simulation fails to reproduce such a linear relation [10,11] and reveals that the contribution from the resonance decay can be either negative or positive depending on the mass [25].

It is noteworthy that a linear dependence between the mean transverse momentum ($\langle p_T \rangle$) and A_{ch} has also been reported in the CMS data [15], i.e.,

$$\Delta \langle p_T \rangle \equiv \langle p_T^- \rangle - \langle p_T^+ \rangle \propto A_{ch}. \qquad (2)$$

The extracted slope of Eq. (2) is found to be consistent in Pb-Pb and p-Pb collisions. It is well known that both v_2 and v_3 linearly depend on p_T. Thus, the relationship between A_{ch} and $\langle p_T \rangle$ can naturally give rise to the dependence between A_{ch} and v_n, serving as a background in the search for the CMW. There are reasons to presume that Eq. (2) is a consequence of the LCC [19]. Few works, however, have quantitatively

*shouqiye@fudan.edu.cn

†mayugang@fudan.edu.cn

established the connection between A_{ch} and p_T in a realistic environment. In this work, we concentrate on the origin of this charge-dependent p_T and investigate the feature of the LCC with the string fragmentation models. We further discuss its impact on the search for the CMW.

II. CHARGE DEPENDENT TRANSVERSE MOMENTUM AND THE LOCAL CHARGE CONSERVATION

The main models used in this analysis include PYTHIA [26,27], DPMJET [28], and HIJING [29]. All of them employ the Lund string fragmentation [30] formalism to deal with the hadronization process, although with different machineries at parton level to construct the color singlet string objects. In the string fragmentation picture, the final state hadrons are produced through the iterative breakups of the string system based on the linear confinement assumption. For a simple string object consisting of a quark and an antiquark endpoints, a new quark-antiquark pair can be created during the string breakup in the middle of two endpoints. They must be produced at the same space-time vertex to meet the requirement of local flavor conservation and then pulled apart by the string tension to form two hadrons. Generally, this process begins with low momentum particles in the central region of the string and then spreads outwards to high momentum particles at later times [30]. In addition to the string fragmentation models, the string melting version of the AMPT model [31], whose initial condition and hadronization are handled by HIJING and a naive quark coalescence respectively, is also adopted as a comparison.

First we examine the A_{ch} dependence of $\langle p_T \rangle$ for positive (h^+) and negative (h^-) hadrons in p-Pb and Pb-Pb collisions at $\sqrt{s_{NN}} = 5.02$ TeV with the aforementioned models. A_{ch} is calculated with all charged hadrons at their final state with $p_T > 0.2$ GeV/c and $|\eta| < 0.8$. A wide p_T coverage of $0.2 < p_T < 5$ GeV/c is applied to estimate $\langle p_T \rangle$, matching the experimental selection criteria. As presented in Figs. 1(a)–1(c), the $\langle p_T \rangle$ of h^+ is systematically larger than that of h^- when $A_{\text{ch}} < 0$ and such a trend reverses when $A_{\text{ch}} > 0$. This feature is qualitatively consistent with the experimental measurement though the relations between A_{ch} and $\langle p_T \rangle$ in the models are not always monotonic. The $\langle p_T \rangle$ difference between h^- and h^+ is calculated and normalized by their average:

$$\Delta \langle p_T \rangle = \frac{p_T^- - p_T^+}{(p_T^- + p_T^+)/2}, \tag{3}$$

to make the apples-to-apples comparison between different systems. In Fig. 1(d), similar linear dependences with a common normalized slope of ≈ 0.1 can be clearly seen in the PYTHIA, DPMJET, and HIJING, which agree perfectly with the CMS measurement.[1] In contrast, no dependence is found in the AMPT model, as marked by the dark grey band. The reason that such a charge (q)-p_T correlation exists in the Lund string family models but not AMPT may be attributed to the fact that, in the AMPT, the spatial charge distribution initially stemming
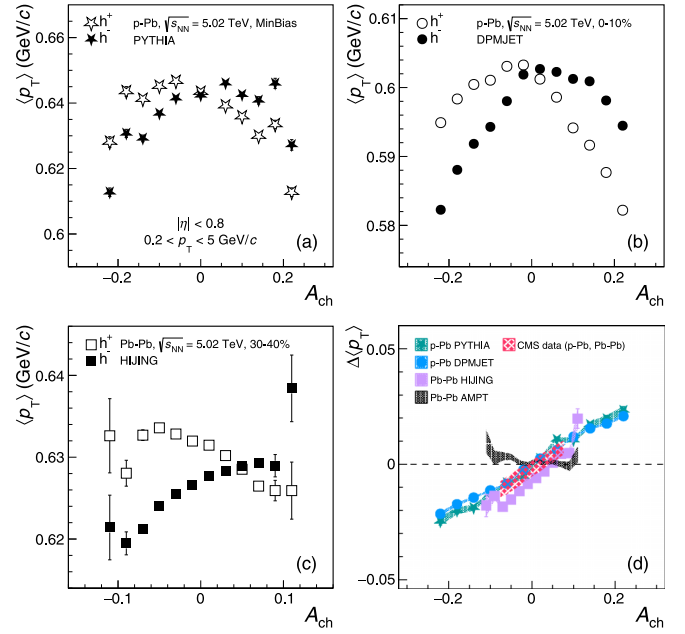
---

[1]The CMS data [15] in p-Pb and Pb-Pb collisions are merged here since they are almost identical.

FIG. 1. Dependence of $\langle p_T \rangle$ (a)–(c) and $\Delta \langle p_T \rangle$ (d) on A_{ch} in Pb-Pb and p-Pb collisions at $\sqrt{s_{NN}} = 5.02$ TeV with different models.

from HIJING is largely distorted during the parton rescattering stage implemented by Zhang's parton cascade (ZPC) model. The q-p_T correlation is therefore no longer guaranteed when the grouped quarks are hadronized to final state particles through coalescence, as proposed in Refs. [32,33].

To understand the intrinsic correlation between q and p_T, the PYTHIA event is dissected and illustrated in Fig. 2. Regardless of collision systems and energies, final state particles originate in either primordial production (labeled A, B, and C) from the string fragmentation (black dashed curves) or the resonance decay (labeled a, b, and c). For the cases of A and a, all particles are emitted within the detector so the total measured charges remain neutral. For the cases of B (C) and b (c), however, more h^+ (h^-) escape from the detector due to the limited acceptance, leading to the charge imbalance. A typical event consists of a few (tens) of each cases and the event A_{ch} can be arithmetically decomposed into the weighted sum of
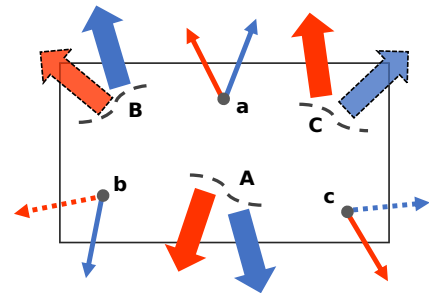

FIG. 2. A schematic view of a PYTHIA event consisting of six production cases. The rectangle denotes the detector in the longitudinal direction. Capital letters denote the string fragmentation while lowercase letters denote the resonance decay with two daughters. Positive and negative charge are marked in red and blue, respectively.
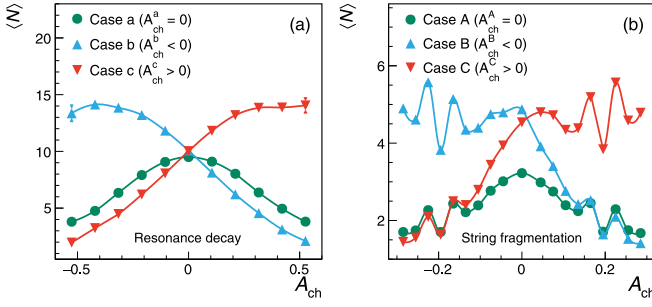
FIG. 3. The average number of each production case (see Fig. 2) as a function of the event A_{ch} in the PYTHIA p-Pb collisions.

TABLE I. Average values of p_T and $|\eta|$ for the detected particles and their mothers in the PYTHIA event.

Type	$\rho^0 \to \pi^+\pi^-$		String frag.	
	unpaired (case b, c)	paired (case a)	unpaired (case B, C)	paired (case A)
Mother p_T	0.75	0.97	0.94	1.41
Mother $|\eta|$	1.17	0.53	2.15	2.12
Daughter p_T	0.59	0.64	0.68	0.74
Daughter $|\eta|$	0.41	0.39	0.41	0.40
Daughter $|\Delta\eta|$	1.27	0.48	1.03	0.69

the charge asymmetry of each case, A_{ch}^i:

$$A_{\mathrm{ch}} = \frac{1}{M} \sum N^i m^i A_{\mathrm{ch}}^i, \qquad (4)$$

where M is the event multiplicity; N^i and m^i are the average number and the average multiplicity of the case i, respectively, and i loop over all six cases. The relation between the event A_{ch} and N is shown in Fig. 3. It can be seen that the event A_{ch} is mainly determined by the numbers of each production case. Apparently, the more cases of B (C) and b (c) one event has, the more negative (positive) the A_{ch} is and vice versa. For those events of $A_{\mathrm{ch}} \approx 0$, the number of B (b) equals that of C (c), counterbalancing the difference between A_{ch}^B and A_{ch}^C, and the proportion of A and a reach the maximum.

As per Eq. (4), the eventwise A_{ch}-$\Delta\langle p_T\rangle$ dependence can be converted into the string and the resonance levels. We start with the contribution from the resonance decay in a given event with $\rho^0 \to \pi^+\pi^-$. Such a typical dynamic process of LCC has proved to be a significant background in the search for the CME [4,9]. In Fig. 4(a), we calculate both A_{ch} and $\Delta\langle p_T\rangle$ with the decayed $\pi^{+/-}$ and find a linear dependence with a positive slope, which is very consistent with the eventwise A_{ch}-$\Delta\langle p_T\rangle$ and the CMS data. This can be easily understood by the following derivation:

$$\Delta\langle p_T\rangle = \frac{p_T^a m^a + p_T^b m^b}{m^a + m^b} - \frac{p_T^a m^a + p_T^c m^c}{m^a + m^c}$$
$$= \frac{m^a (m^c - m^b)(p_T^a - p_T^b)}{(m^a + m^b)(m^a + m^c)}, \qquad (5)$$

where m^i is the multiplicity of case i. Obviously decayed π emitted near the edge of the detector are more likely to be unpaired and carry smaller p_T, i.e., p_T^a (0.64) $> p_T^b \approx p_T^c$ (0.59), as shown in Table I. Thus, for those events of $A_{\mathrm{ch}}^{\mathrm{decay}} <$ ($>$) 0, one has $m^c <$ ($>$) m^b and $\Delta\langle p_T\rangle^{\mathrm{decay}} <$ ($>$) 0. This feature is model independent and simply determined by the fundamental kinematics of the particles.

In the string fragmentation scenario, the parton must carry the opposite charge with its partner for each breakup. As a result, all formed hadrons in an event, excluding the neutral ones, generally have different charges with their local neighbors, which is exactly the manifestation of the LCC as observed in Ref. [14]. The mechanism of Eq. (5), therefore, can be naturally extended to the primordial production as long as one treats each breakup of the string as a resonance. Figure 4(b) presents the local A_{ch}^i-$\Delta\langle p_T\rangle^i$ correlations calculated string by string. Note that B and C only cover half of the A_{ch} since A_{ch}^B and A_{ch}^C are always negative and positive, respectively. An identical linear dependence is found between the stringwise A_{ch}^i-$\Delta\langle p_T\rangle^i$ and the eventwise A_{ch}-$\Delta\langle p_T\rangle$, suggesting the correlation is both global and local. For the same reason, the unpaired primordial hadrons have smaller p_T than the paired ones as listed in Table I. Consequently, as more h^- (h^+) are detected, the more negative (positive) A_{ch} is, and the lower $\langle p_T\rangle^-$ ($\langle p_T\rangle^+$) is. For comparison purposes, we randomly shuffle the charges of particles on the same string, which eliminates the particlewise (local) q-p_T correlation while still preservin the stringwise/eventwise (global) conservation. As expected, the linear dependence vanishes, as shown in the hollow markers of Fig. 4(b).

Table I summarizes the mean p_T, $|\eta|$ for both mothers[2] and daughters, as well as the rapidity separation $|\Delta\eta|$ between two daughters. It is found that the resonances or strings with lower p_T and/or larger $|\eta|$ tend to create unpaired particles with larger $|\Delta\eta|$, leading to the nonzero A_{ch}. This picture agrees with the mechanisms proposed in Ref. [18]. Besides p_T, we also see the linear dependence between $\Delta|\eta|$ and A_{ch}, i.e.,

$$\Delta|\eta| \equiv \langle|\eta^-|\rangle - \langle|\eta^+|\rangle \propto A_{\mathrm{ch}}, \qquad (6)$$

with a negative slope on the order of 10^{-2}, which can be experimentally measured to further examine the LCC.

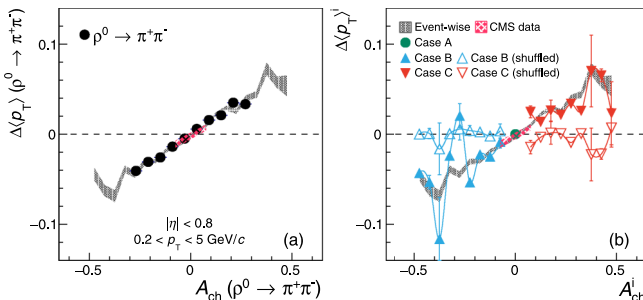
FIG. 4. The local correlation of A_{ch}^i-$\Delta\langle p_T\rangle^i$ from (a) the resonance decay of $\rho^0 \to \pi^+\pi^-$ and (b) the string fragmentation.

_____

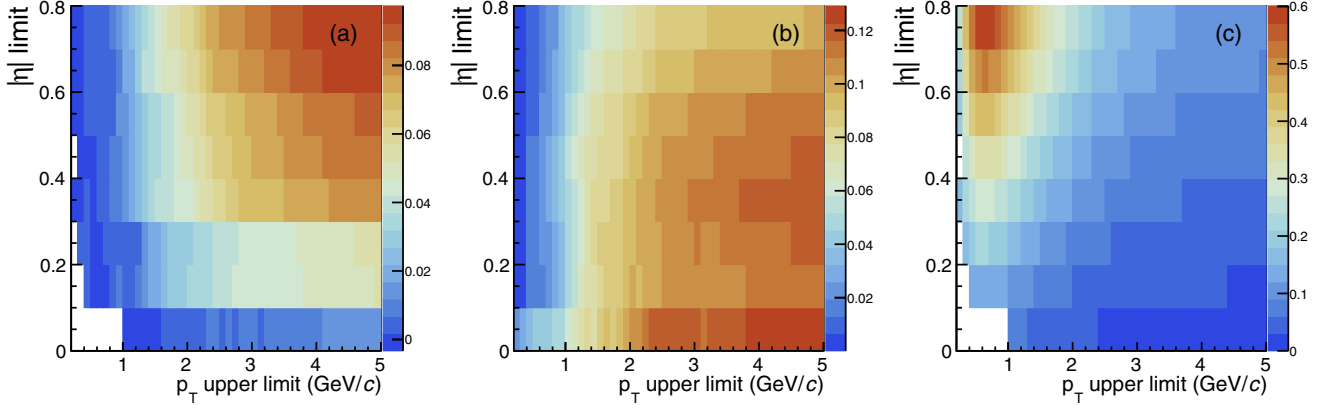[2]Here we define the mother in the string fragmentation as the average of two partons at endpoints.

FIG. 5. The slope values of A_{ch}-$\Delta\langle p_T\rangle$ change with the p_T and $|\eta|$ coverages in the PYTHIA p-Pb collisions. (a) Tuning for both A_{ch} and $\langle p_T\rangle$; (b) $p_T > 0.2$ GeV/c and $|\eta| < 0.8$ are fixed for A_{ch} and only tuned for $\langle p_T\rangle$; (c) $p_T > 0.2$ GeV/c and $|\eta| < 0.8$ are fixed for $\langle p_T\rangle$ and only tuned for A_{ch}.

To sum up, both the resonance decay and the string fragmentation are proven to follow the same pattern and together give rise to the eventwise A_{ch}-$\Delta\langle p_T\rangle$ correlation. Such a relationship is the clear manifestation of the LCC, whose strength depends on the kinematic property of the string/resonance and the size of the detector acceptance.

III. THE IMPACT ON THE SEARCH FOR THE CMW

As demonstrated, when selecting events with a specific A_{ch} value, in practice, one preferentially applies nonuniform p_T and η cuts on the charged particles, resulting in the A_{ch}-Δp_T correlation. This universal background cannot be fully subtracted and needs to be evaluated before extracting the CMW signal. Over the same A_{ch} range, the normalized slope of $\Delta\langle p_T\rangle$ (≈ 0.1) is smaller than that of $\Delta\langle v_2\rangle$ (≈ 0.2–0.3) [15]. Considering that the p_T value is usually larger than v_2 by an order of magnitude, the impact of A_{ch}-Δp_T on A_{ch}-Δv_2 cannot explain the v_2 slope alone. Indeed, a more straightforward behavior of the LCC can be observed in the differential three-particle correlation [14,19].

In the experiment, one may still want to properly select the p_T range to reduce the A_{ch}-Δp_T correlation. Generally, the narrower the p_T range is, the less this effect is included. On the other hand, a wider p_T range enhances particle yields. Hence, we suggest that the integrated v_2 in different A_{ch} bins can be scaled by its $\langle p_T\rangle$ no matter which p_T range is chosen. Moreover, the Δv_2 can be experimentally obtained in two ways: find the p_T-integrated v_n in a given p_T range for h^- and h^+, and then take the difference, or start with the v_n difference between h^- and h^+ as a function of p_T, and then fit the difference in a given range with a constant to get the average. Ideally, these two methods should be consistent; however, in the presence of the already known LCC background, the second way should be more appropriate since it minimizes the Δv_2 induced by $\Delta\langle p_T\rangle$ in each p_T bin and is sensitive to any fluctuation of the $v_2(p_T)$.

The slope caused by the LCC and by the CMW may behave differently in the varied kinematic windows. Figure 5 presents how the slope of A_{ch}-$\Delta\langle p_T\rangle$ changes with the p_T and $|\eta|$ coverages in the PYTHIA model. It can be seen in three panels, respectively, that (a) when narrowing down the upper limits of p_T and $|\eta|$ for both A_{ch} and $\langle p_T\rangle$, the slope is gradually decreased; (b) when $p_T > 0.2$ GeV/c and $|\eta| < 0.8$ are fixed for A_{ch}, the slope is slightly increased as the $|\eta|$ range for $\langle p_T\rangle$ decreases, and decreased as the p_T range for $\langle p_T\rangle$ decreases; and (c) when $p_T > 0.2$ GeV/c and $|\eta| < 0.8$ are fixed for $\langle p_T\rangle$, the slope is dramatically increased by a factor of 6 as the p_T range for A_{ch} decreases to 1 GeV/c, and decreased as the $|\eta|$ range for A_{ch} decreases. If the measured A_{ch}-Δv_2 is merely due to the LCC, one would expect synchronous change between A_{ch}-Δv_2 and A_{ch}-$\Delta\langle p_T\rangle$. By comparison, we directly calculate the A_{ch}-Δv_2 relation with the AMPT model initially imported the quadrupole configuration [10,11] but lacking of the LCC dynamic and find that the slopes only vary moderately in these kinematic windows. It is therefore worthwhile to experimentally compare these slopes to disentangle the LCC- and the CMW-induced A_{ch}-v_2 relations. A preliminary STAR result [13] partially examining the slopes in varied p_T ranges is consistent with our simulation in Fig. 5(b), and further measurements would be more helpful.

Another interesting measurement would be with identified hadrons. The CMW is originally theorized to affect only light quarks [5] and its flavor dependence remains unclear. The slope for kaons is suggested to be negative in Ref. [22] because the isospin chemical potentials between K and π are opposite. It has been tentatively negated, however, by the STAR preliminary data [13]. In the perspective of the LCC, all charged hadrons regardless of species follow the universal A_{ch}-$\Delta\langle p_T\rangle$ correlation. Thus, the slopes of pions, kaons, and protons are expected to be similar and positive (≈ 0.1), as shown in Fig. 6.

One should be aware that the anisotropic flow in PYTHIA and HIJING are very small. This makes it infeasible to directly examine the A_{ch}-v_2 correlation without additional modifications. In contrast, the AMPT model, which succeeds in describing the collectivity, lacks the necessary LCC environment as shown in Fig. 1(d). A recent simulation [34] claims that the HIJING model, when properly scaled, is able to reproduce the behavior of the γ correlator in the CME study.
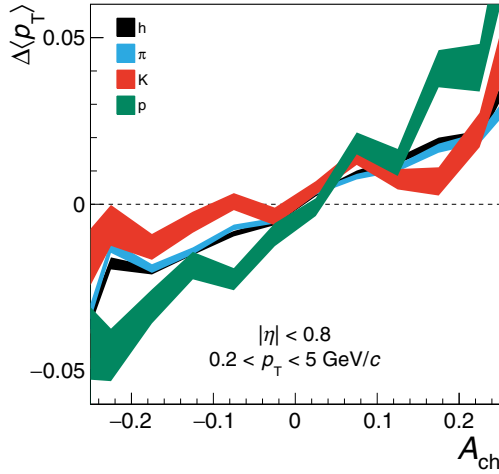
FIG. 6. Dependence of $\Delta\langle p_T\rangle$ on A_{ch} for h, π, K, and p in the PYTHIA simulation.

For this reason, we speculate that the string fragmentation models, when scaled by the correct flow parameters, can also quantitatively describe the experimental measurement of the CMW, which is worth a try in future studies.

IV. SUMMARY

The CMW has been experimentally sought in heavy-ion collisions through the A_{ch} dependence of v_2. Since v_2 linearly depends on p_T, the A_{ch}-dependent $\langle p_T\rangle$ could naturally play a role as a background. With the string fragmentation models, including PYTHIA, DPMJET, and HIJING, we quantitatively reproduce the A_{ch}-$\Delta\langle p_T\rangle$ correlation observed in the data. Such an eventwise correlation can be traced back to the local level. When dissecting the event into different produc-

tion cases (strings and resonances), it is found that the event A_{ch} is mainly determined by the numbers of each case. The key mechanism leading to the q-p_T relation is exactly what the LCC implies; namely, when particles are produced in charge-conserving pairs, the unpaired hadron whose partner is excluded by the limited acceptance usually carries smaller p_T compared to the paired hadrons. As more unpaired h^- (h^+) are detected, the more negative (positive) A_{ch} is, and the lower $\langle p_T\rangle^-$ ($\langle p_T\rangle^+$) is. Both string fragmentation and the resonance decay are proven to follow the same scenario and to generate the similar positive slopes. We argue that when selecting events with a specific A_{ch}, in practice, one preferentially applies nonuniform p_T and η cuts on the charged particles and such a LCC background is too ubiquitous to be fully eliminated. We also propose that measuring the slope of A_{ch}-Δp_T ($\Delta|\eta|$) at varied kinematic windows and with identified hadrons may shed more light on disentangling the difference between the LCC-induced and the CMW-induced A_{ch}-v_2 dependence.

[1] D. E. Kharzeev, L. D. McLerran, and H. J. Warringa, Nucl. Phys. A. **803**, 227 (2008).

[2] D. E. Kharzeev, J. Liao, S. A. Voloshin, and G. Wang, Prog. Part. Nucl. Phys. **88**, 1 (2016).

[3] K. Hattori and X.-G. Huang, Nucl. Sci. Technol. **28**, 26 (2017); Y.-C. Liu and X.-G. Huang, *ibid.* **31**, 56 (2020); J.-H. Gao, G.-L. Ma, S. Pu, and Q. Wang, *ibid.* **31**, 90 (2020).

[4] J. Zhao and F. Wang, Prog. Part. Nucl. Phys. **107**, 200 (2019).

[5] Y. Burnier, D. E. Kharzeev, J. Liao, and H.-U. Yee, Phys. Rev. Lett. **107**, 052303 (2011).

[6] Y. Burnier, D. E. Kharzeev, J. Liao, and H.-U. Yee, arXiv:1208.2537.

[7] H.-U. Yee and Y. Yin, Phys. Rev. C **89**, 044909 (2014).

[8] S. F. Taghavi and U. A. Wiedemann, Phys. Rev. C **91**, 024902 (2015).

[9] F.-Q. Wang and J. Zhao, Nucl. Sci. Technol. **29**, 179 (2018).

[10] G.-L. Ma, Phys. Lett. B. **735**, 383 (2014).

[11] D. Shen, J. Chen, G. Ma, Y.-G. Ma, Q. Shou, S. Zhang, and C. Zhong, Phys. Rev. C **100**, 064907 (2019).

[12] L. Adamczyk *et al.* (STAR Collaboration), Phys. Rev. Lett. **114**, 252302 (2015).

[13] Q.-Y. Shou (STAR Collaboration), Nucl. Phys. A. **982**, 555 (2019); talk given at Quark Matter 2018, https://indico.cern.ch/event/656452/contributions/2869771; H.-j. Xu, J. Zhao, Y. Feng, and F. Wang, Nucl. Phys. A **1005**, 121770 (2021).

[14] J. Adam *et al.* (ALICE Collaboration), Phys. Rev. C **93**, 044903 (2016).

[15] A. M. Sirunyan *et al.* (CMS Collaboration), Phys. Rev. C **100**, 064908 (2019).

[16] V. Khachatryan *et al.* (CMS Collaboration), Phys. Rev. Lett. **118**, 122301 (2017).

[17] R. Belmont and J. L. Nagle, Phys. Rev. C **96**, 024901 (2017).

[18] A. Bzdak and P. Bożek, Phys. Lett. B **726**, 239 (2013).

[19] S. A. Voloshin and R. Belmont, Nucl. Phys. A **931**, 992 (2014).

[20] J. M. Campbell and M. A. Lisa, J. Phys.: Conf. Ser. **446**, 012014 (2013).

[21] M. Stephanov and H.-U. Yee, Phys. Rev. C **88**, 014908 (2013).

[22] Y. Hatta, A. Monnai, and B.-W. Xiao, Nucl. Phys. A **947**, 155 (2016).

[23] M. Hongo, Y. Hirono, and T. Hirano, Phys. Lett. B **775**, 266 (2017).

[24] X.-L. Zhao, G.-L. Ma, and Y.-G. Ma, Phys. Lett. B **792**, 413 (2019).

[25] H.-j. Xu, J. Zhao, Y. Feng, and F. Wang, Phys. Rev. C **101**, 014913 (2020).

[26] T. Sjöstrand, S. Ask, J. R. Christiansen, R. Corke, N. Desai, P. Ilten, S. Mrenna, S. Prestel, C. O. Rasmussen, and P. Z. Skands, Comput. Phys. Commun. **191**, 159 (2015).

[27] T. Sjöstrand, Comput. Phys. Commun. **246**, 106910 (2020).

[28] A. Capella, U. Sukhatme, C.-I. Tan, and J. Tran Thanh Van, Phys. Rep. **236**, 225 (1994); An introduction to DPMJET3, https://wiki.bnl.gov/eic/upload/Dpmjet3_intro.pdf.

[29] M. Gyulassy and X.-N. Wang, Comput. Phys. Commun. **83**, 307 (1994).

[30] S. Ferreres-Solé and T. Sjöstrand, Eur. Phys. J. C **78**, 983 (2018).

[31] Z.-W. Lin, C. M. Ko, B.-A. Li, B. Zhang, and S. Pal, Phys. Rev. C **72**, 064901 (2005).

[32] J. Du, N. Li, and L. Liu, Phys. Rev. C **75**, 021903(R) (2007).

[33] N. Li, Z. Li, and Y. Wu, Phys. Rev. C **80**, 064910 (2009).

[34] J. Zhao, Y. Feng, H. Li, and F. Wang, Phys. Rev. C **101**, 034912 (2020).